Scintigraphic Detection of Pulmonary Aspergillosis in Rabbits with a Radiolabeled Leukotriene B4 Antagonist

Julliëtte E.M. van Eerd, BSc[1]; Huub J.J.M. Rennen, MSc[1]; Wim J.G. Oyen, PhD, MD[1]; Thomas D. Harris, PhD[2]; D. Scott Edwards, PhD[2]; Frans H.M. Corstens, PhD, MD[1]; and Otto C. Boerman, PhD[1]

[1]Department of Nuclear Medicine, University Medical Centre Nijmegen, The Netherlands; and [2]Discovery Research, Bristol-Myers Squibb Medical Imaging, North Billerica, Massachusetts

Radiolabeled chemotactic peptides have been studied for their applicability to the visualization of infectious and inflammatory foci. Because a radiolabeled leukotriene B4 (LTB4) antagonist allowed visualization of intramuscular *E. coli* abscesses in rabbits within a few hours after injection, we decided to test the imaging characteristics of this agent in a more clinically relevant model of pulmonary aspergillosis. The pharmacokinetics and imaging characteristics of the ^{111}In-labeled LTB4 antagonist DPC11870 were studied in New Zealand White rabbits with experimental pulmonary aspergillosis infection. The imaging characteristics of ^{111}In-DPC11870 were compared with those of ^{67}Ga-citrate, a radiopharmaceutical commonly used to detect pulmonary infections in patients. **Methods:** Pulmonary aspergillosis was induced in the left lung of rabbits by intratracheal inoculation of 1×10^8 conidia of *Aspergillus fumigatus*. Three days after the inoculation, the rabbits received ^{111}In-DPC11870 or ^{67}Ga-citrate intravenously. Images were acquired at several time points up to 24 h after injection. **Results:** Pulmonary aspergillosis was visualized with both agents. Images acquired after injection of ^{111}In-DPC11870 showed uptake in the pulmonary lesions from 6 h after injection. Because of accumulation at the site of infection and clearance from the background, the images improved with time. Region-of-interest analysis at 24 h after injection revealed infected lung–to–normal lung ratios of 5.0 ± 1.5 for ^{111}In-DPC11870 and 2.9 ± 0.6 for ^{67}Ga-citrate. **Conclusion:** The radiolabeled LTB4 antagonist DPC11870 clearly delineated experimentally induced pulmonary aspergillosis in rabbits. Images acquired at 24 h after injection of ^{111}In-DPC11870 were superior to those obtained after injection of ^{67}Ga-citrate.

Key Words: LTB4 antagonist; aspergillosis; scintigraphy; ^{67}Ga-citrate

J Nucl Med 2004; 45:1747–1753

Invasive pulmonary aspergillosis (IPA) is a common fungal infection that may affect morbidity and mortality in immunocompromised patients (*1*). Detection of aspergillosis infection at an early stage is of great importance because of the resulting improvement in the therapeutic outcome of patients (*2*). For the diagnosis of IPA, high-resolution chest CT is most often performed. Besides CT, other diagnostic methods, such as fungal culturing and non–culture-based methods such as serodiagnosis or polymerase chain reaction, may be applied (*3*). Scintigraphic imaging techniques may have an additional value in the diagnosis of IPA. They are based on physiologic changes, in contrast to radiologic techniques, which are based on morphologic alterations. ^{67}Ga-Citrate is a radiopharmaceutical commonly used to visualize pulmonary and mediastinal infection, especially for immunocompromised patients in whom low white blood cell (WBC) counts hamper the use of radiolabeled leukocytes (*3*). Several other radiolabeled agents have been studied for applicability to the imaging of infection and inflammation. In particular, radiolabeled chemotactic peptides are promising imaging agents because of their favorable pharmacokinetic characteristics (*4*,*5*). In this study, we investigated the ability of the ^{111}In-labeled leukotriene B4 (LTB4) antagonist DPC11870 to image experimentally induced aspergillosis in New Zealand White (NZW) rabbits.

LTB4 receptors (BLT1 and BLT2) are expressed mainly on leukocytes (*6*). In vitro binding of LTB4 to the BLT receptors results in intracellular signal transduction and subsequent chemotaxis (*7*). LTB4 expression and receptor targeting play an important role in the response of the immune system against infection and inflammation. Furthermore, overproduction of LTB4 contributes to inflammatory diseases, and LTB4 antagonists have been developed to exploit their antiinflammatory effect (*8*). LTB4 targets LTB4 receptors expressed on neutrophilic granulocytes that migrate toward and infiltrate the inflammatory and infectious lesion (*9*). This mechanism of receptor targeting may also be applicable to the visualization of inflammatory and infectious processes by using radiolabeled LTB4 antago-

Received Nov. 18, 2003; revision accepted Apr. 12, 2004.

For correspondence or reprints contact: Julliëtte E.M. van Eerd, BSc, Department of Nuclear Medicine, University Medical Center Nijmegen, P.O. Box 9101, 6500 HB Nijmegen, The Netherlands.

E-mail: j.vaneerd@nucmed.umcn.nl

nists. In this study, a bivalent LTB4 antagonist was labeled with ^{111}In, and its ability to allow visualization of pulmonary aspergillosis in NZW rabbits was compared with that of ^{67}Ga-citrate.

MATERIALS AND METHODS

DPC11870

Synthesis of the compound was based on the polyethylene glycol–tethered LTB4 antagonist SG385 described in a previous report (*10*). Boc-cysteic acid and Boc-Glu(OTfp)-OTfp were prepared as previously described (*11,12*). All other reagents were purchased from Aldrich Chemical Corp. or Fluka Chemical Corp.

The tetra-cysteic acid derivative of SG385 was prepared by the sequential coupling of Boc-cysteic acid in dimethylformamide using benzotriazol-tetramethyluronium-hexafluorophosphate coupling reagent. Boc was removed by treatment with 50:50 trifluoroacetic acid:methylene chloride. Purifications were performed after the addition of the first cysteic acid (partitioning between $CHCl_3$ and water) and after the addition of the second and fourth cysteic acids (high-performance liquid chromatography [HPLC] on C18 silica using 0.1% trifluoroacetic acid–modified acetonitrile/water mobile phases). Products were recovered from HPLC mobile phases by lyophilization. The tetra-cysteic acid derivative 11870 was checked with HPLC and high-resolution mass spectrometry. In addition, the dimerization was achieved by reaction of 11870 with the bis-trifluoropropanone ester of Boc-glutamic acid and hydroxyazabenzotriazole (HOAt) in dimethylformamide. The crude reaction product was treated with trifluoroacetic acid/methylene chloride/triethylsilane to remove the Boc protecting group. The product was purified with C18 HPLC in a 0.1 mol/L ammonium acetate–modified acetonitrile/water mobile phase. Conjugation with diethylenetriaminepentaacetic acid was accomplished by reaction with diethylenetriaminepentaacetic acid anhydride in dimethylformamide. Purification gave DPC11870 in 73% yield from intermediate DPC11870. HPLC analysis of the lyophilized product gave a single peak. Additional quality control was performed with ^{1}H nuclear magnetic resonance, and performance of high-resolution mass spectrometry showed an (M + 2H) value of 1563.5056 for this $C_{123}H_{182}N_{26}O_{53}S_8$ structure.

Radiolabeling of DPC11870

DPC11870 was labeled with $^{111}InCl_3$ in metal-free 0.25 mol/L ammonium acetate buffer, pH 5.5, for 30 min at room temperature. Radiochemical purity was checked by instant thin-layer chromatography (R_f of ^{111}In-DPC11870, 0–0.5; R_f of unbound ^{111}In, 1.0) and by reversed-phase HPLC on a C18 column (Zorbax Rx-C18, 4.6 mm × 25 cm; Agilent Technologies) as described previously (*13*).

^{67}Ga-Citrate

^{67}Ga-Citrate was commercially obtained (DRN 3103; Tyco Healthcare). The activity concentration was 37 MBq/mL at calibration time.

Aspergillus fumigatus

A. fumigatus, used for the induction of the infection, was isolated from an immunocompromised patient diagnosed with an *A. fumigatus* infection. The inoculum was prepared from a frozen isolate that was subcultured 2 times onto Sabouraud dextrose agar slants, followed by an incubation period of 5 d at 30°C. Conidia were harvested with phosphate-buffered saline (Invitrogen BV; Gibco) containing 0.20% Tween 20 (Sigma-Chemical Co.). Conidia were washed 3 times in Hanks' balanced salt solution without calcium and magnesium (BioWhittaker Europe) and transferred to a 50-mL conical tube and counted in a hemocytometer. The concentration was adjusted to give each rabbit a predetermined inoculum of 1×10^8 conidia of *A. fumigatus* in a volume of 250 μL.

Induction of Pulmonary Aspergillosis

Fourteen female NZW rabbits weighing 2.3–2.8 kg were used during the experiments. Animals were housed individually and fed standard laboratory chow and water ad libitum. All animal experiments were approved by the local animal welfare committee in accordance with the Dutch legislation and performed in accordance with their guidelines.

Twelve rabbits received cytarabine (cytosine arabinoside) injections to bring about immunosuppression, using a modification of a method to induce neutropenia in rabbits (*14*). Cytarabine injections were given on 4 consecutive days to lower the WBC counts and allow the aspergillosis infection to become established. The other 2 animals remained healthy and served as control animals (for comparison with the pharmacokinetics of ^{111}In-DPC11870 in cytarabine-treated animals) (Table 1). Aspergillosis was induced essentially as described by Groll et al., with a few modifications for our application (*14*). Cytarabine (Onco-Tain; Faulding Pharmaceuticals nv) was administered intravenously (525 mg/m^2) on days −4 through −1 before the injection of radiolabeled compound. On day −3, after the second dose of cytarabine, *A. fumigatus* conidia were inoculated in 10 animals. Two animals injected with cytarabine were not inoculated and served as a second control group. Before inoculation, the animals were sedated with a subcutaneous injection of 0.7 mL of Hypnorm (fentanyl, 0.315 mg/mL, plus fluanisone, 10 mg/mL; Janssen Pharmaceutical). During inoculation, the rabbits received inhalation anesthesia with a mixture of isoflurane, nitrous oxide, and oxygen and were placed on the operation table. The inoculum of 1×10^8 conidia (250 μL) was given intratracheally into the left lung, together with 50 μL of 5% Evans blue dye (E2129; Sigma-Aldrich) via a syringe attached to a polyethylene 0.76 × 1.22 mm catheter (PE tube; Maxxim Medical).

Imaging and Biodistribution

At day 0 (3 d after inoculation of *A. fumigatus*), 9 rabbits (2 healthy, 2 injected with cytarabine only, and 5 both injected with cytarabine and infected with *A. fumigatus*) received an injection of 11 MBq of ^{111}In-DPC11870 (3 μg) via the ear vein. The other 5 animals pretreated with cytarabine and infected with *A. fumigatus* received 11 MBq of ^{67}Ga-citrate intravenously. Images (300,000 counts per image) were acquired immediately after injection of the radiolabeled preparations and at 2, 4, 6, and 24 h after injection. For scintigraphic imaging, the rabbits were immobilized in a mold and placed prone on the medium-energy parallel-hole collimator of the γ-camera in the anterior position (Orbiter; Siemens). Images were stored digitally in a 256 × 256 matrix. All images were windowed identically, allowing a fair comparison of the images acquired during the various experiments. The scintigraphic results were analyzed using regions of interest (ROI) drawn over the abscess and the contralateral noninfected lung (normal). Ratios of infected lung to normal lung (infected-to-normal ratios) were calculated. At 24 h after injection, all rabbits were euthanized with a lethal dose of sodium pentobarbital and organs were dissected. A blood sample was taken by cardiac puncture and tissues were

TABLE 1
Schematic Overview of Animal Experiments

Rabbit no.	Days					
	−4	−3	−2	−1	0	1
1–5: group A	Blood Cytarabine	Induction Aspergillosis + cytarabine	Cytarabine	Cytarabine	Blood ^{111}In-DPC11870 + imaging	Imaging + biodistribution
6–10: group B	Blood Cytarabine	Induction Aspergillosis + cytarabine	Cytarabine	Cytarabine	Blood ^{67}Ga-Citrate + imaging	Imaging + biodistribution
11–12: group C	Blood Cytarabine	Cytarabine	Cytarabine	Cytarabine	Blood ^{111}In-DPC11870 + imaging	Imaging + biodistribution
13–14: group D	Blood				Blood ^{111}In-DPC11870 + imaging	Imaging + biodistribution

Blood samples were taken on day −4 and 0 to determine WBC count. Animals were injected with cytarabine on days −4 through 0, and aspergillosis was induced on day −3. At day 0, animals were injected with ^{111}In-DPC11870 (groups A, C, and D) or ^{67}Ga-citrate. Animals of group C were not inoculated with aspergillosis, and animals from group D were not injected with aspergillosis or cytarabine.

weighed and the amount of radioactivity measured to determine the biodistribution of both agents. The activity in tissues was measured in a shielded well-type γ-counter (Wizard; Pharmacia-LKB) together with the injection standards. Radioactivity concentration was expressed as percentage injected dose per gram (%ID/g).

Hematologic and Histopathologic Studies

Blood samples were collected from all rabbits, both at day −4 before the first cytarabine injection and at day 0 (time of injection of the radiolabel), to determine the WBC count of the animals.

During dissection of the animals, samples of the infected (left) and noninfected lung were aseptically removed. One part of each lung sample was cultured for *A. fumigatus* for 24 h at 37°C on Sabouraud dextrose agar plates. A second specimen of lung tissue was fixed in phosphate-buffered formalin. After measurement of radioactivity, these tissues were embedded in paraffin. Tissue sections were stained with hematoxylin–eosin or Grocott methenamine silver and histopathologically examined.

Statistical Analysis

All values are presented as mean ± SD. Statistical analysis was performed using the 2-sided Student *t* test. The level of significance was set at 0.05.

RESULTS

Radiolabeling of DPC11870

Quality control tests by reversed-phase HPLC analysis and instant thin-layer chromatography indicated that the radiochemical purity exceeded 99%. The specific activity was 3.7 MBq of DPC11870 per microgram (12 MBq/nmol).

A. fumigatus

Culturing of the conidia solution confirmed that the inoculum consisted of *A. fumigatus* conidia. Animals infected with *A. fumigatus* began to show clinical symptoms 2 d after conidia inoculation. Respiration was more frequent and shallower in infected animals than in control animals. Intake of water and food was normal.

Hematologic and Histopathologic Studies

The mean WBC concentration of the rabbits at the time of the first cytarabine injection (day −4) was 13.5 ± 5.7 × 10^9/L. Four days after cytarabine administration, the WBC concentration of these rabbits was significantly reduced (5.2 ± 2.4 × 10^9/L, $P = 0.0036$). Normal WBC counts in NZW rabbits vary between 5.0 and 11.0 × 10^9/L (*15*). The WBC counts after induction of aspergillosis and injection of cytarabine indicated that the rabbits were not persistently neutropenic, but the numbers were much lower than on the first day of the experiment (day 0).

At dissection, all animals inoculated with *A. fumigatus* showed macroscopic infectious lesions in the lungs. In all but 1 rabbit, the infected area of lung corresponded to the area marked with Evans blue. In 1 rabbit (injected with ^{111}In-DPC11870), the infection had affected both lungs. Culture of *A. fumigatus* was positive in 3 of 5 animals injected with ^{67}Ga-citrate. In 3 of the 5 cases in which animals were injected with ^{111}In-DPC11870 and inoculated with *A. fumigatus* conidia, positive cultures were found (1 of these animals showed positive cultures in both lungs). One animal was positive only for staphylococcus species. Both lungs from the 4 control rabbits and the remainder lung tissues (control lungs not inoculated with *A. fumigatus*) were negative after culturing.

Histologic examination of tissue sections of the healthy animals showed no signs of infection; that is, infiltration of macrophages or granulocytes was absent (Fig. 1A). The sections of lungs infected with *A. fumigatus* conidia showed massive infiltration of mainly granulocytes (Fig. 1B). Staining with Grocott methenamine silver revealed truncated *A. fumigatus* hyphae and germinating conidia in all animals that were inoculated with *A. fumigatus* conidia (Fig. 1D). Staining of the tissue samples obtained from healthy lungs was negative for aspergillosis (Fig. 1C).

Imaging and Biodistribution

The scintigraphic images acquired immediately and at 2, 4, 6, and 24 h after injection of ^{111}In-DPC11870 or ^{67}Ga-citrate are shown in Figure 2. Immediately after injection, rabbits injected with ^{111}In-DPC11870 showed uptake of radioactivity in heart, lung, liver, and kidneys (Fig. 2A). At

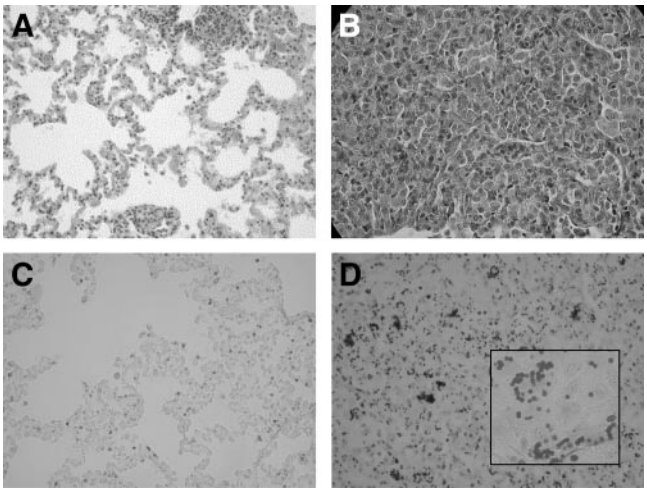

FIGURE 1. Histologic sections of healthy lung tissue (A and C) and lung tissue with IPA (B and D) from NZW rabbits. Hematoxylin–eosin staining (A and B) shows massive infiltration of polymorphonuclear cells in the infected lung tissue. Grocott methenamine silver staining (C and D) indicates the presence of *A. fumigatus* hyphae and germinating conidia in the infected lung tissue. (A–D, ×200; inset in D, ×400)

later times, accumulation of activity was seen in spleen and bone marrow. The radioactivity concentration in the heart (circulation) and in the lungs decreased with time. The infectious area in the lungs first became visible at 6 h after injection, after radioactivity had lessened in the normal lung tissue and circulation and had accumulated in the infectious foci. Images obtained at 24 h after the injection of the radiolabeled LTB4 antagonist showed an even more evident clearance of radioactivity from noninfected lung areas. This continuous clearance in combination with ongoing accumulation of radioactivity in the infected lung tissue resulted in distinct visualization of the lung lesions at 24 h after injection of the radiolabel. The images showed that, except for the kidneys, activity concentration in the remainder of the body was low.

Images acquired at several times after injection of ^{67}Ga-citrate showed distinct pharmacokinetics for this compound, as compared with ^{111}In-DPC11870 (Fig. 2B). Immediately after injection, ^{67}Ga-citrate distributed to the different organs and high activity concentrations were seen in the kidneys and bladder. ^{67}Ga first revealed pulmonary infection at 2 h after injection. The pulmonary lesion was visible as a small focal spot in the left lung. At that moment, uptake of ^{67}Ga in the bone was also present. In contrast to images obtained with the ^{111}In-LTB4 antagonist, all ^{67}Ga-citrate images obtained more than 2 h after injection remained similar.

Region-of-interest analysis of the normal and infected lung areas showed that, after injection of ^{111}In-DPC11870, infected-to-normal ratios increased at a constant rate throughout the experiment (Fig. 3). The ratios for ^{67}Ga-citrate increased during the interval 0–4 h after injection but remained constant at later times. At 24 h after injection, the ratios for ^{67}Ga-citrate images were 1.7-fold lower than those for ^{111}In-DPC11870 images (5.0 ± 1.5 and 2.9 ± 0.6 for ^{111}In-DPC11870 and ^{67}Ga-citrate, respectively, $P = 0.020$).

Biodistribution data (24 h after injection) derived from ex vivo counting of dissected tissues are presented in Figure 4. Uptake of ^{111}In-DPC11870 in infected lung tissue at the time of biodistribution was very high. Uptake of radioactivity was 16-fold higher in infected lung tissue than in normal lung tissue (0.82 %ID/g vs. 0.05 %ID/g, respectively, $P = 0.008$). Relatively high uptake of the compound was also measured in bone marrow and spleen. Biodistribution data obtained with ^{67}Ga-citrate were concordant with the images, and the highest radioactivity concentration of

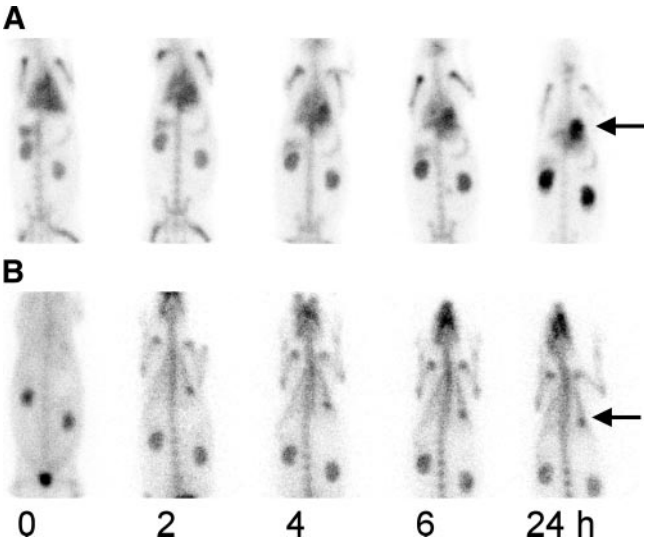

FIGURE 2. Scintigraphic images of NZW rabbits with pulmonary aspergillosis. The rabbits received 11 MBq of ^{111}In-DPC11870 (A) or ^{67}Ga-citrate (B) intravenously. Anterior images were acquired immediately and at 2, 4, 6, and 24 h after injection of the radiolabel. Arrows indicate focus of infection.

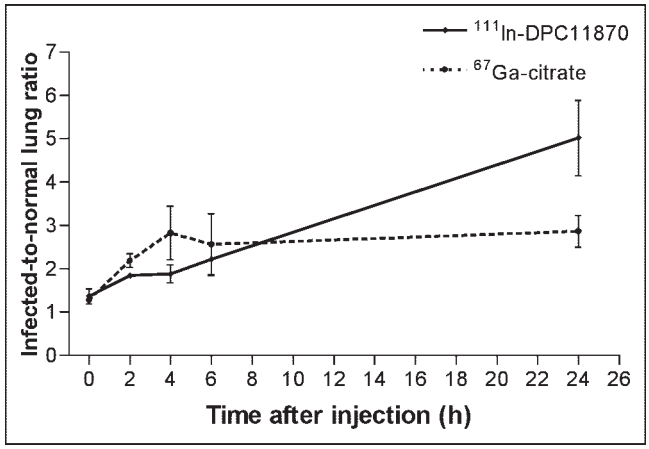

FIGURE 3. Plot of infected-to-normal ratios vs. time after injection of ^{111}In-DPC11870 ($n = 5$) or ^{67}Ga-citrate ($n = 5$) in NZW rabbits with pulmonary aspergillosis. Region-of-interest analysis from images acquired at several time points after injection gave the ratios. Error bars indicate SD.

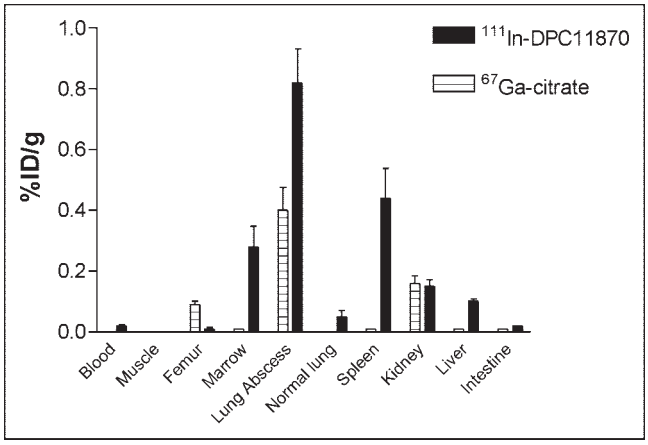

FIGURE 4. Biodistribution data obtained 24 h after injection of ^{111}In-DPC11870 (n = 5) and ^{67}Ga-citrate (n = 5) in NZW rabbits with pulmonary aspergillosis. Error bars indicate SD.

this radiopharmaceutical was measured in infected lung tissue. As noticed on the images, the radioactivity concentration of ^{67}Ga-citrate was relatively high in the bone and in the kidneys. In contrast to the derived ROI ratios, the infected-to-normal ratio calculated from the biodistribution data at 24 h after injection was significantly (4.1-fold) higher for ^{67}Ga-citrate than for ^{111}In-DPC11870 (P = 0.0005).

To determine whether the cytarabine injections affected the pharmacokinetics and biodistribution pattern of the radiolabeled LTB4 antagonist, noninfected control animals were included in this study. Images acquired immediately after injection of ^{111}In-DPC11870 appeared similar in all groups. Figure 5 shows 24-h-postinjection images of a cytarabine-treated, *A. fumigatus*–infected animal; a cytarabine-treated, noninfected animal; and a healthy rabbit injected with ^{111}In-DPC11870. Rabbits not infected with *A. fumigatus* conidia (either untreated or treated with cytarabine) did not show any accumulation or retention of radioactivity in the lungs. Furthermore, the biodistribution of ^{111}In-DPC11870 in the main organs of these animals (except bone marrow and spleen) was comparable to that in cytarabine-treated, infected rabbits. Distinct differences in radioactivity concentrations were observed in the spleen and bone marrow of healthy animals and animals with aspergillosis. The cytarabine-treated animals showed reduced uptake of ^{111}In-DPC11870 in these organs.

Quantitative measurement of radioactivity revealed that, except for the bone marrow and spleen, concentrations in dissected organs did not significantly differ between the rabbits (healthy or infected) treated with cytarabine and the healthy, untreated animals (Fig. 6). The radioactivity concentration in the bone marrow was lower for cytarabine-treated animals (both infected and noninfected) (0.28% ± 0.15 %ID/g and 0.38% ± 0.20 %ID/g, respectively) than for healthy animals (0.93% ± 0.13 %ID/g). The radioactivity concentration in the noninfected lungs of all 3 groups of animals was similar. Also, the ^{111}In-DPC11870 concentration in the blood of rabbits from all 3 groups was similar (0.02% ± 0.01 %ID/g in rabbits with aspergillosis, 0.01% ± 0.02 %ID/g in rabbits healthy but treated, and 0.03% ± 0.01 %ID/g in rabbits healthy and not treated with cytarabine).

DISCUSSION

In the present study, scintigraphic imaging of pulmonary aspergillosis with a radiolabeled LTB4 antagonist was examined in a rabbit model. The imaging potential of the LTB4 antagonist was compared with that of ^{67}Ga-citrate. Serial scintigraphic images showed that with ^{111}In-DPC11870, the pulmonary infection could be seen from 6 h onward. The images showed that the radiolabeled LTB4 antagonist accumulated in the infectious lesion, whereas the activity concentration in the blood and normal lung tissue decreased with time. The pharmacokinetic properties of the

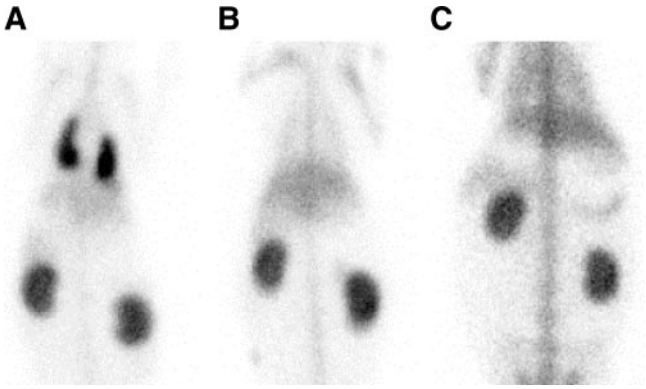

FIGURE 5. Anterior images acquired 24 h after injection of ^{111}In-DPC11870 in a NZW rabbit with pulmonary infection in both lungs (A), a noninfected animal treated with cytarabine (B), and a rabbit neither infected with *A. fumigatus* nor treated with cytarabine (C).

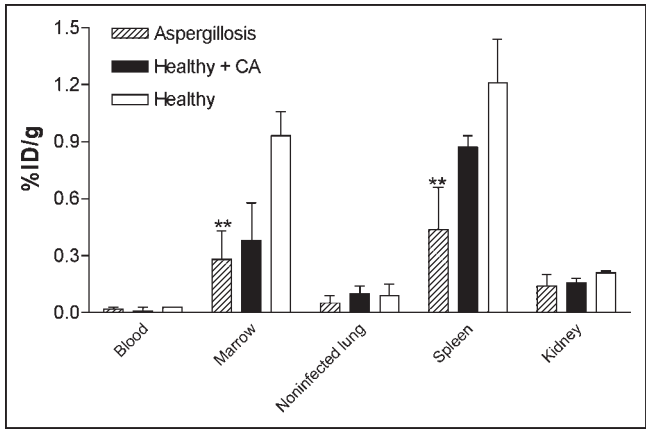

FIGURE 6. Biodistribution data obtained 24 h after injection of ^{111}In-DPC11870 in NZW rabbits with pulmonary infection in the lung (n = 5), cytarabine (CA)-treated noninfected animals (n = 2), and healthy rabbits neither injected with cytarabine nor infected with *A. fumigatus* (n = 2). Error bars indicate SD. $^{**}P <$ 0.05; results differ significantly from results in healthy rabbits.

compound in this model were concordant with results found in previous studies (*13*). Injection of the compound in healthy animals showed that except for the amount of radioactivity in bone marrow and spleen, localization of ^{111}In-DPC11870 was not affected by administration of cytarabine). This finding implies that despite the lowered WBC counts in the circulation, sufficient activated neutrophils migrated to the site of infection. No differences were seen in radioactivity concentration in the blood and the major organs. The lower amounts of radioactivity in the spleen and bone marrow of animals pretreated with cytarabine were probably due to the reduced number of premature WBCs in these organs. Cytarabine is a nucleoside analog with cytotoxic activity mainly affecting replicating cells (*16*). The lower radioactivity concentration in the bone marrow may be due to the fact that repeated injection of cytarabine will immediately reduce the numbers of proliferating (LTB4 receptor–positive) promyelocytes in the bone marrow, whereas mature and activated neutrophils will be less affected and would require longer treatment with this antimetabolite. This is in agreement with the massive infiltration of leukocytes found in the infected lung tissue of these rabbits (histologic staining).

The primary aim of this study was to test whether the radiolabeled LTB4 antagonist ^{111}In-DPC11870 could allow visualization of pulmonary aspergillosis in NZW rabbits. In addition, we compared the imaging and biodistribution characteristics of ^{111}In-DPC11870 with those of ^{67}Ga-citrate, the radiopharmaceutical generally used to visualize pulmonary infections in patients (*17*). Besides the relatively high sensitivity for acute and chronic infection and inflammation, a few other disadvantages of ^{67}Ga-citrate include the relatively long biologic half-life, physiologic uptake in bone, and excretion via the bowel (the last mainly at later times) (*18*). Images acquired after injection of ^{67}Ga-citrate in rabbits with *A. fumigatus* infection clearly delineated the infected lesions in the lungs at early times. Physiologic uptake in the bone was first seen on images 2 h after injection, and the amount of radioactivity did not decrease with time. Region-of-interest analysis indicated that the infected-to-normal ratios found with ^{111}In-DPC11870 increased with time (in contrast to the ratios found after injection of ^{67}Ga-citrate) and resulted in higher ratios for ^{111}In-DPC11870 than for ^{67}Ga-citrate at 24 h after injection of the radiolabeled agents. The increasing infected-to-normal ratios after injection of the radiolabeled LTB4 antagonist can be explained by the continuous accumulation of radioactivity at the site of infection in combination with ongoing clearance from the blood (corresponding to background). ^{67}Ga-Citrate cleared more quickly from the circulation than did ^{111}In-DPC11870; therefore, at later time points the ratios remained constant. Normally, regions of interest on images are evaluated to diagnose pulmonary infection. Physiologic uptake of ^{67}Ga-citrate in the bone (background tissue) deteriorated the images and reduced the infected-to-normal ratios derived from region-of-interest analysis. Our data indicate that although pulmonary lesions are visualized, that visualization may be affected by physiologic uptake. This outcome may be more pronounced in patients, especially because images are generally acquired at 18–72 h after the injection of ^{67}Ga-citrate (*19,20*).

In this study, we showed that ^{111}In-DPC11870 allowed clear visualization of pulmonary aspergillosis in rabbits. Visualization was possible because of accumulation of radioactivity in the infection. In a previous study, we determined that this accumulation is specific and receptor mediated (*13*). Because of the massive infiltration of granulocytes in the infectious foci and accumulation of ^{111}In-DPC11870 in the lesions, this model represents acute pulmonary infection, and presumably, ^{111}In-DPC11870 might allow visualization of acute pulmonary infection in general. Because uptake of ^{111}In-DPC11870 in the bone marrow and retention of radioactivity in the kidneys could limit the clinical applicability of the compound, we now aim to produce a new analog of the LTB4 antagonist DPC11870 that can be labeled with ^{99m}Tc. A ^{99m}Tc-labeled compound not only could reduce the absorbed dose to these organs but also might improve images because of the higher resolution and reduced visualization of bone marrow (due to higher attenuation by the bone). Nevertheless, because of the distinct visualization of pulmonary lesions made possible by injection of ^{111}In-DPC11870, this agent could be a valuable tool for the diagnosis of acute pulmonary infections in patients.

CONCLUSION

The present study demonstrated that the radiolabeled LTB4 antagonist DPC11870 allows visualization of pulmonary infection in rabbits with aspergillosis. Visualization of lesions began 6 h after injection and improved with time because of retention of radioactivity in the infected lung tissue. The results of this study indicate that ^{111}In-DPC11870 could contribute to the diagnosis of acute pulmonary infection.

ACKNOWLEDGMENTS

The authors thank Gerry Grutters, Margo van den Brink, and Maichel van Riel (University of Nijmegen, Central Animal Laboratory) for technical assistance and microbiologic analysis.

REFERENCES

1. Hauggaard A, Ellis M, Ekelund L. Early chest radiography and CT in the diagnosis, management and outcome of invasive pulmonary aspergillosis. *Acta Radiol.* 2002;43:292–298.
2. Becker MJ, Dams ET, de Marie S, et al. Scintigraphic imaging using ^{99m}Tc-labeled PEG liposomes allows early detection of experimental invasive pulmonary aspergillosis in neutropenic rats. *Nucl Med Biol.* 2002;29:177–184.
3. Kontoyiannis DP, Bodey GP. Invasive aspergillosis in 2002: an update. *Eur J Clin Microbiol Infect Dis.* 2002;21:161–172.
4. Onuffer JJ, Horuk R. Chemokines, chemokine receptors and small-molecule antagonists: recent developments. *Trends Pharmacol Sci.* 2002;23:459–467.
5. van der Laken CJ, Boerman OC, Oyen WJ, et al. Technetium-99m-labeled

chemotactic peptides in acute infection and sterile inflammation. *J Nucl Med.* 1997;38:1310–1315.
6. Toda A, Yokomizo T, Shimizu T. Leukotriene B4 receptors. *Prostaglandins Other Lipid Mediat.* 2002;68–69:575–585.
7. Ford-Hutchinson AW. Leukotriene B4 in inflammation. *Crit Rev Immunol.* 1990;10:1–12.
8. Engels F, Nijkamp FP. Pharmacological inhibition of leukotriene actions. *Pharm World Sci.* 1998;20:60–65.
9. Serhan CN, Prescott SM. The scent of a phagocyte: advances on leukotriene B(4) receptors. *J Exp Med.* 2000;192:F5–F8.
10. Barrett JA, Cheesman EH, Harris TD, Rajopadhye M, inventors; Bristol Meyer Squibb, assignee. Radiopharmaceuticals for imaging infection and inflammation. PCT Int Appl WO 9815295 A2. 1998.
11. Hubbuch A, Danho W, Zahn H. Synthesis of N-protected cysteic acid derivatives and their activated esters. *Liebigs Ann Chem.* 1979:776–783.
12. Harris TD, Barrett JA, Carpenter AP, Rajopadhye M, inventors; Bristol Meyer Squibb, assignee. Vitronectin receptor antagonist pharmaceuticals. US patent 6511649 B1. 2003.
13. van Eerd JEM, Oyen WJG, Harris TD, et al. A bivalent leukotriene B4 antagonist for scintigraphic imaging of infectious foci. *J Nucl Med.* 2003;44:1087–1091.
14. Groll AH, Gonzalez CE, Giri N, et al. Liposomal nystatin against experimental pulmonary aspergillosis in persistently neutropenic rabbits: efficacy, safety and non-compartmental pharmacokinetics. *J Antimicrob Chemother.* 1999;43:95–103.
15. Hematology of laboratory and miscellaneous animals. In: Jain NC, ed. *Schalm's Veterinary Hematology.* Vol 91. Philadelphia, PA: Lea and Febiger; 1986:275–298.
16. Johnson SA. Clinical pharmacokinetics of nucleoside analogues: focus on haematological malignancies. *Clin Pharmacokinet.* 2000;39:5–26.
17. Seabold JE, Palestro CJ, Brown ML, et al. Procedure guideline for gallium scintigraphy in inflammation. *J Nucl Med.* 1997;38:994–997.
18. Boerman OC, Dams ET, Oyen WJ, Corstens FH, Storm G. Radiopharmaceuticals for scintigraphic imaging of infection and inflammation. *Inflamm Res.* 2001;50:55–64.
19. Sugawara Y, Gutowski TD, Fisher SJ, Brown RS, Wahl RL. Uptake of positron emission tomography tracers in experimental bacterial infections: a comparative study of radiolabeled FDG, thymidine, L-methionine, ^{67}Ga-citrate and ^{125}I-HAS. *Eur J Nucl Med.* 1999;26:333–341.
20. Alazraki NP. Gallium-67 imaging in infection. In: *Principles and Practice of Nuclear Medicine*. 2nd ed. St. Louis, MO: Mosby-Year Book; 1995:702–713.